A seismologically consistent compositional model of Earth's core

James Badro[a,b,1], Alexander S. Côté[a,c], and John P. Brodholt[c]

[a]Institut de Physique du Globe de Paris, Sorbonne Paris Cité–Université Paris Diderot, Unité Mixte de Recherche 7154, Centre National de la Recherche Scientifique, 75005 Paris, France; [b]Earth and Planetary Sciences Laboratory, École Polytechnique Fédérale de Lausanne, CH-1015 Lausanne, Switzerland; and [c]Department of Earth Sciences, University College London, London WC1E 6BT, United Kingdom

Edited by Ho-kwang Mao, Carnegie Institution of Washington, Washington, DC, and approved April 14, 2014 (received for review September 4, 2013)

Earth's core is less dense than iron, and therefore it must contain "light elements," such as S, Si, O, or C. We use ab initio molecular dynamics to calculate the density and bulk sound velocity in liquid metal alloys at the pressure and temperature conditions of Earth's outer core. We compare the velocity and density for any composition in the (Fe–Ni, C, O, Si, S) system to radial seismological models and find a range of compositional models that fit the seismological data. We find no oxygen-free composition that fits the seismological data, and therefore our results indicate that oxygen is always required in the outer core. An oxygen-rich core is a strong indication of high-pressure and high-temperature conditions of core differentiation in a deep magma ocean with an FeO concentration (oxygen fugacity) higher than that of the present-day mantle.

mineral physics | first principles | geophysics

From the analysis of iron meteorites and the observation of Earth's moment of inertia, we know that the primary constituent of Earth's core is an iron alloy (1) with Fe/Ni~16 (2, 3). Comparing seismic travel times in the core with experimental shockwave measurements, Birch (1) proposed that the core is lighter than pure iron. Shockwave and static diamond anvil cell (DAC) experiments have further constrained the core's density deficit (with respect to pure iron) to be between 5 and 10% (4). This requires lower atomic weight elements to be present as additional constituents—so-called light elements. Moreover, the density jump at the inner core boundary (ICB) between the solid inner core and liquid outer core is ~4.5% (5), too large to be due to just the solid–liquid phase transition, and indicates that the outer core contains more light elements (~5–10%) than the inner core (~2–3%). The prime light-element candidates for the core, taking into account cosmochemical and petrological constraints, are silicon, sulfur, carbon, oxygen, and hydrogen (6). Models for core composition allow in principio a mixture of several light elements, and many arguments have been put forward over the years for and against each of the elements (2, 7, 8).

Silicon, sulfur, and carbon are rather soluble in iron at all conditions and were originally quite sensibly proposed as the most valid candidates. They are compatible with low-pressure core formation models, either in a shallow magma ocean or in the differentiated accretionary material. The solubility of these elements in molten iron coexisting with silicate melt would be several percent (9), even at low pressures. On the other hand, oxygen solubility is much more limited at low pressures, and DAC experiments show that oxygen can be introduced in the core by reaction with the molten mantle at high pressures and temperatures (10, 11). Oxygen thus became a natural candidate with the introduction of the "deep magma ocean" models (12–15) of core formation. Additional support for oxygen in the core comes from the fact that oxygen is the only light element to be highly incompatible in solid iron; therefore most of the oxygen would be expelled from the growing inner core and remain in the outer core (7, 8), hence elegantly accounting for the problem of the large density contrast between the inner and outer core. Hydrogen is extremely volatile and is thought to have been brought to Earth during late accretion (16, 17), after the core had formed. In this case, it would be essentially nonexistent in the proto-Earth during core formation and not a likely candidate for the light element in the core.

The literature offers a wide range (3, 2, 7, 8, 10, 11, 18, 19) of plausible estimates for the light-element composition of the core (*SI Appendix*, section 1). To constrain these further, we need to assess whether the compositional model for the core matches the seismically observed density and sound velocity of the core. As the core is 95% molten, this analysis has not been possible due to the lack of density and velocity data on (Fe–Ni)–C–O–Si–S liquid alloys under core conditions. Measuring bulk sound velocities and densities in molten Fe alloys at core conditions lies currently beyond the capability of experimentation. An alternative is to use ab initio simulations to interpret seismic observations (20) in terms of outer core composition. We therefore calculated the density and bulk sound velocity of liquid alloys in the (Fe–Ni)–C–O–Si–S system using ab initio molecular dynamics. We then compared the properties of the molten alloys directly with the primary geophysical observations [e.g., density and bulk sound velocity obtained (21) from radial seismic models]. This allowed us to identify the subset of compositions that match the constraints and, finally, to propose a seismologically constrained compositional model of Earth's core.

The simulations were performed on liquid iron binaries ($Fe_{1-x}Ni_x$; $Fe_{1-x}C_x$; $Fe_{1-x}O_x$; $Fe_{1-x}Si_x$; $Fe_{1-x}S_x$) at two different concentrations (x = 8.3 and 16.7 mol%) at the pressure and temperature conditions of the core–mantle boundary (CMB) and the ICB (on the outer core side). Details about the simulations can be found in the *SI Appendix*, section 2.

We calculated the densities with a statistical uncertainty (1σ) of 0.15% and bulk sound velocities with a statistical uncertainty

Significance

It is well known that Earth's core is made primarily of iron, alloyed with ~5% nickel and some lighter elements, such as carbon, oxygen, silicon, or sulfur. The amount as well as the chemistry of the light elements is poorly known and still a matter of considerable debate. In this paper we calculate the seismic signature of iron-rich light-element alloys and compare them to the seismic properties of Earth's core. We find that oxygen is required as a major light element in the core, whereas silicon, sulfur, and carbon are not required. We also find that silicon concentration in the core cannot be higher than 4.5%, and sulfur concentration cannot be higher than 2.4%.

Author contributions: J.B., A.S.C., and J.P.B. designed research; J.B., A.S.C., and J.P.B. performed research; J.B., A.S.C., and J.P.B. analyzed data; and J.B. and J.P.B. wrote the paper.

The authors declare no conflict of interest.

This article is a PNAS Direct Submission.

[1]To whom correspondence should be addressed. E-mail: badro@ipgp.fr.

This article contains supporting information online at www.pnas.org/lookup/suppl/doi:10.1073/pnas.1316708111/-/DCSupplemental.

(1σ) of 0.8%. These are reported in Fig. 1. We combined the binary data assuming ideal mixing to obtain the density and bulk sound speed for any composition in the (Fe–Ni)–C–O–Si–S system as $\rho = \sum x_i \rho_i$ and $V_\Phi = \sqrt{\frac{K}{\rho}}$ where $\frac{1}{K} = \sum \frac{x_i}{K_i}$. ρ is the density of the mixture, K its bulk modulus, V_Φ its bulk sound velocity, and x_i, ρ_i, and K_i, are the volume fraction, density, and bulk modulus of the Fe–X_i component, respectively. Ideal mixing has been the standard working hypothesis in this kind of study (6, 19, 22) and will need to be verified by future work. However, our study reinforces this hypothesis by showing that (*i*) the binary systems are perfectly ideal (as can be seen by the perfectly linear fits of density versus concentration) and (*ii*) our calculations were compared with existing shockwave data (19, 22–24) on molten Fe, Fe–O, and Fe–S alloys and found them to be in excellent agreement (*SI Appendix*, section 3). It should also be noted that high-pressure experiments have shown that miscibility gaps vanish at high pressures (25–28), hence also indicating that high-density liquids tend to have a simpler thermodynamic behavior than their low-pressure counterpart.

We calculated ρ_{CMB}, ρ_{ICB}, $V_{\phi,CMB}$, and $V_{\phi,ICB}$ for various outer core compositional models in the literature, derived from both experimental and theoretical models (2, 7, 8, 10, 11). These are reported in Fig. 1, alongside the binary data. Except for the ab initio model of Alfè et al. (7), all of the models overestimate the concentration of light elements, yielding densities that are too low. The velocities for the various core compositions are generally higher than observed at the CMB, another indication that the light-element concentration was overestimated.

Assuming a chemically homogeneous outer core, we can constrain its composition by finding all possible combinations of light-element concentrations for which their densities and velocities match those of the Preliminary Reference Earth Model simultaneously at the CMB and ICB. The Fe/Ni ratio in chondrites shows very little variance, so we fix Fe/Ni at 16 (2, 3). The CMB temperature is fixed at T_{CMB} = 4,300 K so that the ICB temperature (calculated along the isentrope) is T_{ICB} = 6,300 K (*SI Appendix*, section 2), which is consistent with iron melting at the ICB (6, 29). The results for other temperature profiles are also tested. We generated over 100 million combinations of (x_O, x_{Si}, x_S, x_C), never exceeding a threshold of 25 mol% for any single light element, and calculated their densities and bulk sound velocities. We kept the compositions that satisfy the four seismological constraints (ρ_{CMB}, ρ_{ICB}, $V_{\phi,CMB}$, $V_{\phi,ICB}$) while propagating all uncertainties (0.15% on calculated densities, 0.5% on seismic densities, 0.8% on calculated velocities, and 0.2% on seismic velocities) in our multicomponent model to obtain a seismologically constrained core compositions.

The first striking observation is that all of our solutions contain oxygen, and there are no solutions in an oxygen-free system. Second, there is a valid core composition with oxygen being the only light element (5.4 ± 0.4%) [all percentages are in weight (wt%) except where otherwise noted], alloyed with Fe–Ni. No other element is able to satisfy the constraints alone. Finally, the maximum concentrations permissible for silicon and sulfur concentrations are rather low, 4.5 and 2.4%, respectively. To visualize the complex solution space, we first plotted the ternary solution spaces: (Fe–Ni)–O–Si, (Fe–Ni)–O–C, and (Fe–Ni)–O–S in

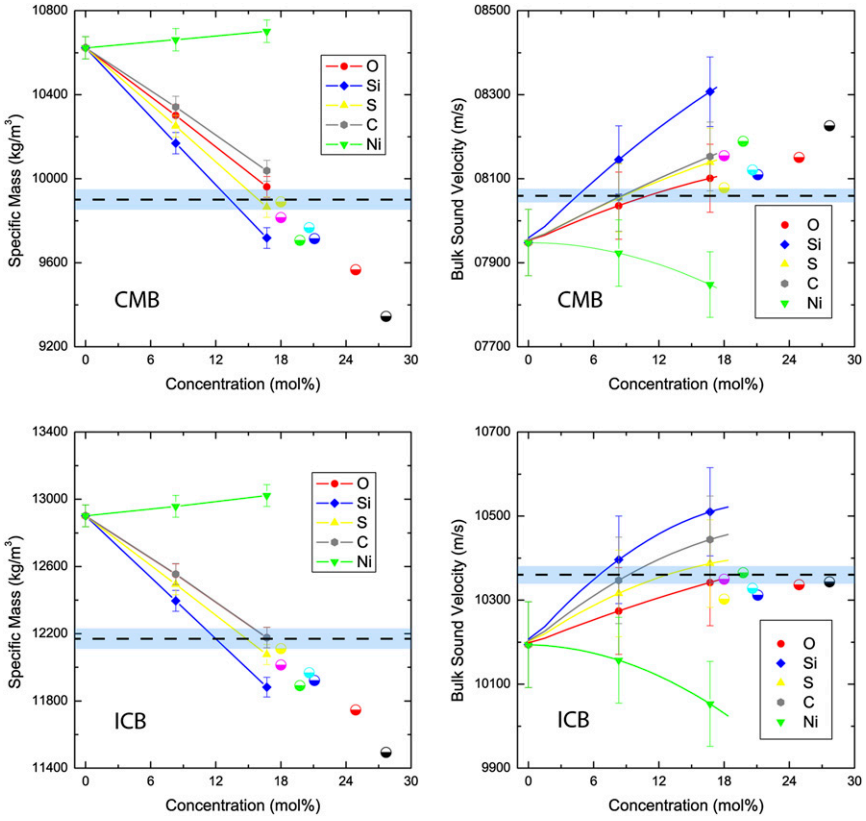

Fig. 1. Density (*Left*) and bulk sound velocity (*Right*) of molten Fe-Ni, Fe-C, Fe-O, Fe-Si, and Fe-S alloys as a function of concentration at CMB (*Upper*) and ICB (*Lower*) conditions. The calculations are represented by full symbols, and the lines are fits to the data (density, linear; bulk sound velocity, quadratic). Note that the densities of C and O at the ICB overlap and are indistinguishable. The horizontal dashed line represents the seismological "target value," and the shaded area represents its uncertainty. The half-filled circular points are the calculated density and bulk sound velocity for various core compositional models proposed in the literature—black (2), red (10), blue (11), green (8), purple, Si from ref. 7; light blue, S from ref. 7.

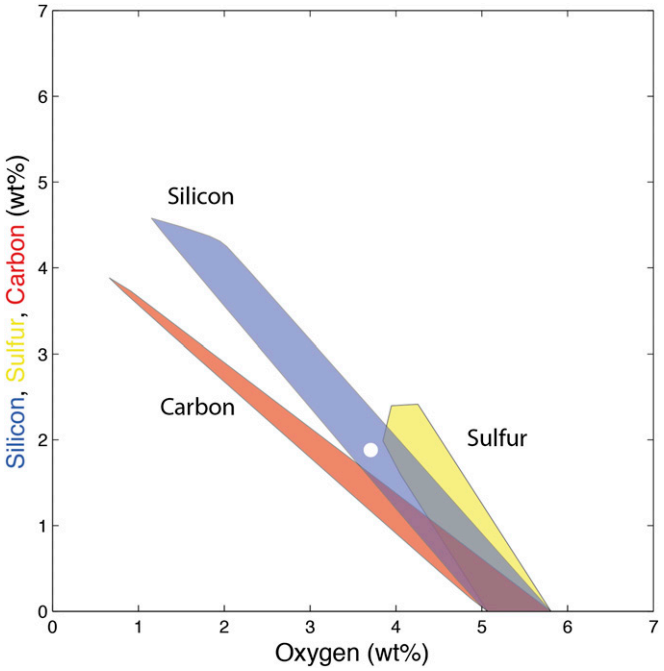

Fig. 2. Range of core compositions compatible with seismic observations. Each shaded area represents the ternary solution space that satisfies the seismic density and bulk sound velocity at the top and bottom of the outer core ($Fe_{94}Ni_6$–O–Si, blue; $Fe_{94}Ni_6$–O–C, red; and $Fe_{94}Ni_6$–O–S, yellow). There is no solution for the other ternaries ($Fe_{94}Ni_6$–Si–S, $Fe_{94}Ni_6$–Si–C, and $Fe_{94}Ni_6$–S–C). This shows that oxygen is always required to match the seismic data. The best numerical fit is shown by the white circle corresponding to 3.7% O, 1.9% Si, 0% S, and 0% C.

Fig. 2 [the other three ternaries, (Fe–Ni)–Si–S, (Fe–Ni)–Si–C, and (Fe–Ni)–S–C, have no solution]. From all those acceptable compositions, we have calculated the best numerical solution: it is a core that contains 3.7% O, 1.9% Si, and no sulfur or carbon (*SI Appendix*, Table S2), a composition indicated by a white circle in Fig. 2.

We can further constrain our compositional model by using inner-core compositional models and experimental metal–silicate partitioning data. Recent studies have proposed that the inner core is a Fe–Ni–Si alloy containing between 1 and 2% silicon (8, 30). Because the inner core is growing from the outer core, and these are in chemical equilibrium, then the outer core should also contain silicon, between 1.2 and 3.6% [assuming a liquid/solid partition coefficient (7) of 1.5 ± 0.3 for silicon]. Moreover, core formation experiments place a tight constraint (12, 31–35) on oxygen solubility in molten iron: incorporating large amounts of oxygen in a core-forming metal in equilibrium with a molten silicate requires very high temperatures. In those conditions, silicon will always be incorporated in the metal as well (31, 34, 35).

With oxygen being required from outer-core seismology and silicon being required from inner-core seismology as well as metal–silicate partitioning, our model leaves little room for other light elements such as sulfur and carbon. This is in agreement with recent results obtained by first principles' simulations of metal–silicate equilibrium (36). These suggest that the main core components are Si and O, whereas volatile element contents such as C and H lie well below the 1% and 1,000 ppm threshold, respectively. We therefore focused our attention on the (Fe–Ni)–O–Si system and evaluated the influence of varying S and C contents on the final Si and O content. We plotted the (Fe–Ni)–O–Si solution space calculated when incorporating carbon (0, 0.2, and 1%) and/or sulfur (0, 1, and 2%) in Fig. 3. As expected, adding S and/or C in the core reduces the range of acceptable O–Si concentrations as major elements and has a more pronounced effect on oxygen rather than silicon. However, the picture remains qualitatively the same, and oxygen is always required in the core.

All these results are based on a core–mantle boundary temperature of 4,300 K, a condition that was chosen so that the inner-core boundary temperature (calculated along the isentrope) falls on the melting temperature of iron (6, 29). To verify that our solution is robust, we checked the sensitivity to temperature. We performed the same calculations for a range of CMB temperatures from 3,800 to 4,700 K, with ICB temperatures ranging from 5,500 to 6,900 K, respectively. The calculations are reported in the *SI Appendix*, sections 5 and 6. Higher temperatures make for less light elements, and conversely, a core at lower temperature requires more light elements. The solution spaces shift to higher or lower concentrations with T, but the general topology of the solution, and our conclusions, remains unchanged.

This study shows that oxygen is present, and likely in high concentrations, in the outer core. Because the solubility of oxygen in iron requires high temperatures and high FeO concentration (oxygen fugacity) in coexisting silicate melts, our observation strongly favors models of core formation in a deep magma ocean

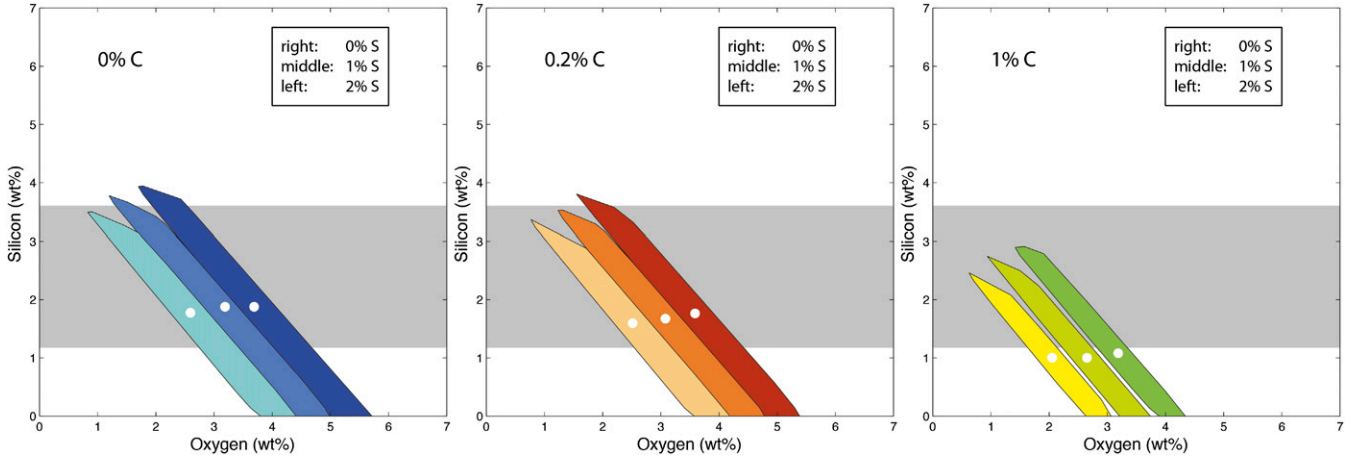

Fig. 3. Range of O and Si compositions compatible with seismic observations, calculated for varying S and C concentrations. Each panel corresponds to a fixed carbon content: (*Left*) 0% C; (*Center*) 0.2% C; (*Right*) 1% C. In each panel, we calculate three sulfur concentrations: dark (0% S), light (1% S), and lighter (2% S). For each of the nine S–C combinations plotted, we calculate the best numerical fit represented by a white circle. The horizontal gray band represents the outer-core silicon concentration range required by inner-core models (7, 8, 30).

(35) under relatively oxidizing conditions (magma ocean FeO content higher than that of the present-day mantle) or by merging of several large protoplanets that have experienced such conditions (37, 38). A core with high oxygen content is consistent with inner-core models (8, 30) and helps explain the large density contrast at the ICB. It has been proposed that oxygen (33) is a light element whose presence in the core dramatically changes the activity of V and Cr during metal–silicate equilibrium, modifying their partition coefficients to reach concentrations in the mantle in accord with geochemical observation, as long as the core contains 3–6% oxygen (34, 35); such contents fall in the range of our solutions. Combining the geophysical constraints (from this work) with geochemical constraints (siderophile trace-element partitioning) should be a very effective tool to further constrain core formation scenarios as well as the chemical environment that prevailed during terrestrial accretion.

ACKNOWLEDGMENTS. The research leading to these results has received funding from the European Research Council (ERC) under the European Community's Seventh Framework Programme (FP7/2007-2013)/ERC Grant Agreement 207467. We acknowledge the use of HECToR, the UK national high-performance computing service on which these calculations were performed.

1. Birch F (1952) Elasticity and constitution of the Earth's interior. *J Geophys Res* 57(2): 227–286.
2. Allegre CJ, Poirier JP, Humler E, Hofmann AW (1995) The chemical composition of the Earth. *Earth Planet Sci Lett* 134(3–4):515–526.
3. McDonough WF, Sun SS (1995) The composition of the Earth. *Chem Geol* 120(3–4): 223–253.
4. Anderson DL (2002) The case for irreversible chemical stratification of the mantle. *Int Geol Rev* 44(2):97–116.
5. Shearer P, Masters G (1990) The density and shear velocity contrast at the inner core boundary. *Geophys J Int* 102(2):491–498.
6. Poirier JP (1994) Light elements in the Earth's outer core: A critical review. *Phys Earth Planet Inter* 85(3–4):319–337.
7. Alfè D, Gillan MJ, Price GD (2002) Composition and temperature of the Earth's core constrained by combining ab initio calculations and seismic data. *Earth Planet Sci Lett* 195(1–2):91–98.
8. Badro J, et al. (2007) Effect of light elements on the sound velocities in solid iron: Implications for the composition of Earth's core. *Earth Planet Sci Lett* 254(1–2): 233–238.
9. Jana D, Walker D (1997) The impact of carbon on element distribution during core formation. *Geochim Cosmochim Acta* 61(13):2759–2763.
10. Sakai T, et al. (2006) Interaction between iron and post-perovskite at core-mantle boundary and core signature in plume source region. *Geophys Res Lett* 33(15):L15317.
11. Takafuji N, Hirose K, Mitome M, Bando Y (2005) Solubilities of O and Si in liquid iron in equilibrium with (Mg,Fe)SiO3 perovskite and the light elements in the core. *Geophys Res Lett* 32(6):L06313.
12. Rubie DC, Gessmann CK, Frost DJ (2004) Partitioning of oxygen during core formation on the Earth and Mars. *Nature* 429(6987):58–61.
13. Rubie DC, Melosh HJ, Reid JE, Liebske C, Righter K (2003) Mechanisms of metal-silicate equilibration in the terrestrial magma ocean. *Earth Planet Sci Lett* 205(3–4):239–255.
14. Wood BJ, Walter MJ, Wade J (2006) Accretion of the Earth and segregation of its core. *Nature* 441(7095):825–833.
15. Drake MJ, Righter K (2002) Determining the composition of the Earth. *Nature* 416(6876):39–44.
16. Wood BJ, Halliday AN, Rehkämper M (2010) Volatile accretion history of the Earth. *Nature* 467(7319):E6–E7.
17. Albarede F, et al. (2013) Asteroidal impacts and the origin of terrestrial and lunar volatiles. *Icarus* 222(1):44–52.
18. Alfè D, Price GD, Gillan MJ (1999) Oxygen in the Earth's core: A first-principles study. *Phys Earth Planet Inter* 110(3-4):191–210.
19. Huang HJ, et al. (2011) Evidence for an oxygen-depleted liquid outer core of the Earth. *Nature* 479(7374):513–516.
20. Stixrude L, Wasserman E, Cohen RE (1997) Composition and temperature of Earth's inner core. *J Geophys Res Solid Earth* 102(B11):24729–24739.
21. Dziewonski AM, Anderson DL (1981) Preliminary reference Earth model. *Phys Earth Planet Inter* 25(4):297–356.
22. Huang HJ, et al. (2013) Shock compression of Fe-FeS mixture up to 204 GPa. *Geophys Res Lett* 40(4):687–691.
23. Brown JM, McQueen RG (1986) Phase transitions, Grüneisen parameters and elasticity for shocked iron between 77 GPa and 400 GPa. *J Geophys Res* 91:7485–7494.
24. Nguyen JH, Holmes NC (2004) Melting of iron at the physical conditions of the Earth's core. *Nature* 427(6972):339–342.
25. Sanloup C, Fei Y (2004) Closure of the Fe-S-Si liquid miscibility gap at high pressure. *Phys Earth Planet Inter* 147(1):57–65.
26. Tsuno K, et al. (2007) In situ observation and determination of liquid immiscibility in the Fe-O-S melt at 3 GPa using a synchrotron X-ray radiographic technique. *Geophys Res Lett* 34(17):L17303.
27. Corgne A, Wood BJ, Fei Y (2008) C- and S-rich molten alloy immiscibility and core formation of planetesimals. *Geochim Cosmochim Acta* 72(9):2409–2416.
28. Morard G, Katsura T (2010) Pressure-temperature cartography of Fe-S-Si immiscible system. *Geochim Cosmochim Acta* 74(12):3659–3667.
29. Anzellini S, Dewaele A, Mezouar M, Loubeyre P, Morard G (2013) Melting of iron at Earth's inner core boundary based on fast X-ray diffraction. *Science* 340(6131): 464–466.
30. Antonangeli D, et al. (2010) Composition of the Earth's inner core from high-pressure sound velocity measurements in Fe-Ni-Si alloys. *Earth Planet Sci Lett* 295(1–2):292–296.
31. Ricolleau A, Fei Y, Corgne A, Siebert J, Badro J (2011) Oxygen and silicon contents of Earth's core from high pressure metal-silicate partitioning experiments. *Earth Planet Sci Lett* 310(3–4):409–421.
32. Frost DJ, et al. (2010) Partitioning of oxygen between the Earth's mantle and core. *J Geophys Res Solid Earth* 115:B02202.
33. Corgne A, Siebert J, Badro J (2009) Oxygen as a light element: A solution to single-stage core formation. *Earth Planet Sci Lett* 288(1–2):108–114.
34. Siebert J, Badro J, Antonangeli D, Ryerson FJ (2013) Terrestrial accretion under oxidizing conditions. *Science* 339(6124):1194–1197.
35. Siebert J, Badro J, Antonangeli D, Ryerson FJ (2012) Metal-silicate partitioning of Ni and Co in a deep magma ocean. *Earth Planet Sci Lett* 321:189–197.
36. Zhang YG, Yin QZ (2012) Carbon and other light element contents in the Earth's core based on first-principles molecular dynamics. *Proc Natl Acad Sci USA* 109(48):19579–19583.
37. Raymond SN, O'Brien DP, Morbidelli A, Kaib NA (2009) Building the terrestrial planets: Constrained accretion in the inner Solar System. *Icarus* 203(2):644–662.
38. Raymond SN, Quinn T, Lunine JI (2006) High-resolution simulations of the final assembly of Earth-like planets I. Terrestrial accretion and dynamics. *Icarus* 183(2): 265–282.

Supporting Information

1. Compositional Models in the Literature

Models in the literature propose a large range of plausible core compositions. Using cosmochemical trends and geochemical (mantle) data, Allegre *et al.*(1) concluded that the core contains 7.4% Si, 2.3% S and 4.1% O. From DAC experiments, Takafuji *et al.*(2) concluded that the outer core contains ~3% O and ~6% Si as light components, whereas Sakai *et al.*(3) suggested that at core-mantle boundary conditions, up to 4% Si and 6.3% O can be dissolved into molten Fe. From sound velocities measurements in the DAC, Badro *et al.*(4) proposed an outer core model containing 2.8% of Si, 5.3% O, and very little S. Conversely, a shockwave study by Huang *et al.*(5) proposed the opposite and claimed that the core must contain very little, or even no oxygen. In parallel to the experimental efforts, first-principles calculations based on density functional theory (DFT) have been successfully applied to study the properties of Fe and its alloys under extreme conditions. Alfe *et al.*(6) suggested that the outer core may contain 2.5±0.8% O and also 5-7% Si and/or S (with unconstrained proportions). On the basis of siderophile trace-element partitioning between core and mantle, Corgne *et al.*(7) suggested the core contains 3 to 6 wt% oxygen, and Siebert *et al.*(8) propose that the core should contain 2 to 5 wt% oxygen.

2. Calculations

The molecular dynamics (MD) simulations were carried out in the NVT-canonical ensemble, using VASP(9), which incorporates the projected augmented wave (PAW) method(10) to represent the electron orbitals. We used well-mixed binaries of 108 atoms, using the super-cell approach and Γ-point sampling. The simulations were first well mixed at very high temperatures, before gradually reducing them to the desired temperature. The simulations were run for a period of ~13-15 ps, with a time step of 1 fs, in order to obtain adequate statistics and reliable pressures (between 0.1 and 0.2 GPa, using the blocking method to estimate uncertainties(11)) at a given volume (see Figure S1).

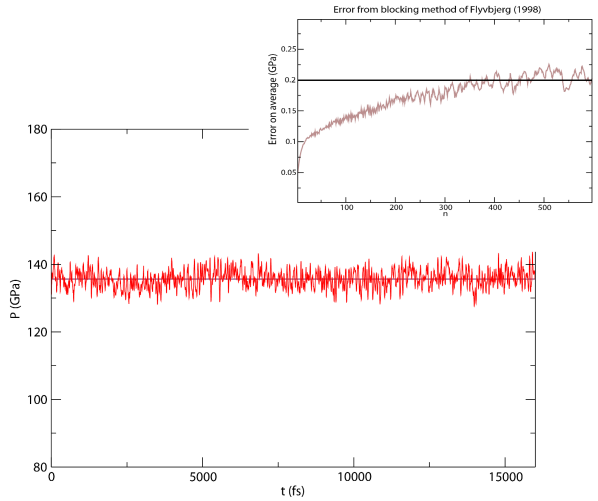

Figure S1. An example of the pressure variation during the simulation for pure Fe, together with an analysis of the statistical error on the mean. The average pressure is 136 +/- 0.2 GPa.

Following the MD simulation, a set of snapshots was taken from each run and a calculation on each of these was performed with high cut-off energy of 800 eV and a dense k-point grid, in order to evaluate the average Pulay stress. The Pulay stress varied from system to system

but was no more than 6.5 GPa. GGA calculations on Fe are known to slightly underestimate the pressure and this must be corrected with experimental data. By comparing lattice dynamics calculations of solid iron(12) to high pressure and temperature experiments along the Hugoniot(13), we evaluated the pressure correction to be 10 GPa at the CMB and 8 GPa at the ICB. The quasi-harmonic lattice dynamics results were in turn validated by running molecular dynamics simulations at different pressures along the Hugoniot; the agreement between the two methods was 1 GPa or less. Moreover we show below (Section 3) that when using this pressure correction our densities on liquid Fe agree well within error with results based on new shockwave data of Huang *et al.*(5)

The bulk sound velocity is a function of density and adiabatic bulk modulus:

$$V_\phi = \sqrt{\frac{K_S}{\rho}}$$

We considered 11 composition: $Fe_{1-x}Ni_x$; $Fe_{1-x}C_x$; $Fe_{1-x}O_x$; $Fe_{1-x}Si_x$; $Fe_{1-x}S_x$ (where x = 0 ; 0.083 ; 0.167). For each composition, we calculated the density at core-mantle boundary (CMB) and the inner-core boundary (ICB) pressures and temperatures; We also relaxed a set of 6 volumes bracketing CMB and ICB pressures by 10 GPa. These were then fit to a Birch-Murnaghan equation of state in order to obtain the isothermal bulk modulus at core pressures and temperatures:

$$K_T = -V \cdot \left(\frac{\partial P}{\partial T}\right)_T$$

We also performed simulations at different temperatures for two volumes surrounding the CMB and ICB, from which we calculated the thermal expansion coefficient $\alpha_{CMB} = 1.95 \cdot 10^{-5}$ K^{-1} and $\alpha_{ICB} = 1.15 \cdot 10^{-5}$ K^{-1} and the Grüneisen parameter $\gamma_{CMB} = 1.54$ and $\gamma_{ICB} = 1.43$. Assuming an adiabatic outer core, we calculated the relationship between the temperatures at the CMB and ICB, using the relationship:

$$T_{ICB} = T_{CMB} \cdot \exp\left(\int_{P_{CMB}}^{P_{ICB}} \frac{\gamma}{K_S} dP\right)$$

The integral was calculated assuming a linear variation of γ between P_{CMB} and P_{ICB}, and the adiabatic bulk modulus was obtained by:

$$K_S = K_T \cdot (1 + \alpha\gamma T)$$

We ran the simulations at a slightly higher temperature than the ones assumed for the core: 4800 K at the CMB and 6500 K at the ICB. The densities were then corrected to the desired temperature according to:

$$\Delta\rho = \alpha\rho\Delta T$$

3. Comparison with Experiments

In order to check the validity of our calculations, we compared them with the available experimental data, *i.e.* shockwave measurements on liquid Fe(13) and $Fe_{0.74}S_{0.03}O_{0.23}$ and $Fe_{0.85}S_{0.08}O_{0.07}$ alloys(5). Even if the temperature is unconstrained in many shockwave experiments, we can compare the data in density-velocity space, where temperature effects are implicitly integrated in density (table S1) following to Birch's law. We calculated densities and bulk sound velocities for the three experimentally studied composition using our calculations and mixing model. For pure liquid Fe, our ICB point (330 GPa) is literally identical to the shockwave data (table S1), showing that our standard state (pure molten iron) is a very good proxy for the real system.
For Fe-S-O alloys, we reproduce the available density-velocity data at the CMB and at the ICB. The agreement at the CMB is quite impressive for both density and velocity (table S1). Density is very well reproduced at the ICB, whereas velocities show an increased discrepancy, but are still within error bars (table S1). These two independent experimental comparisons bring necessary and strong validations of our numerical data. Also, this shows that the ideal mixing hypothesis used in our model is consistent with experiments, when they are available. If ideal mixing was not a valid hypothesis, we would not be able to match the experiments in ternary systems with our calculations in binary systems.

Sample	Ref.	P (GPa)	ρ (kg/m³)	+/-	Δρ	V (m/s)	+/-	ΔV
Fe	B&M 1986	333	12920	40	19	10190	40	4
	This Work	330	12901	19		10194	102	
$Fe_{0.74}S_{0.03}O_{0.23}$	H 2011	135	9683	150	96	8288	330	133
	This Work	130	9587	62		8155	82	
	H 2011	330	11742	180	28	10994	430	591
	This Work	330	11770	77		10403	104	
$Fe_{0.85}S_{0.08}O_{0.07}$	H 2011	135	9985	150	25	8099	390	14
	This Work	130	9960	65		8113	81	
	H 2011	330	12119	180	59	10878	520	518
	This Work	330	12178	79		10360	104	

Table S1: *Comparison between our calculations and shockwave experiments (B&M-1986(13) and H-2011(5)). The comparison goes by 2-line series with the experimental data first, and our calculations second. P is pressure in GPa, ρ is density in kg/m³, and V bulk sound speed in m/s. "Δρ" and "ΔV" are the density and bulk sound velocity difference between each experiment and the corresponding calculations. Except for one point (in red), all the differences are smaller than the error bars and are identical within the accuracy of the measurement and calculation.*

4. Error Propagation and Statistical Robustness

We use our calculations to predict the density and bulk sound velocity of any melt in the Fe-Ni-C-O-Si-S system. The densities and sound velocities are calculated at 135 GPa (corresponding to the pressure at the CMB) and at 330 GPa (pressure at the ICB). For each composition corresponds a set of 4 values: ρ_{CMB}, ρ_{ICB}, $V_{\phi,CMB}$, and $V_{\phi,ICB}$ and these are

compared to PREM values at the same pressure. Only the compositions for which all four values match PREM are considered, hence returning a seismologically consistent composition for the entire outer core. For each composition, we have a certain mismatch, and we calculated the one that has the lowest mismatch with respect to seismology; this is reported in Table S1. Interestingly, this "best match" is always S- and C- free, and consists of Fe-Ni-O-Si. The statistical uncertainties of the measurements and observations are 0.5% (seismology) and 0.15% (calculations) on density, and 0.2% (seismology) and 0.8% (calcualtions) on velocity. We obtain our solution space by propagating all theses uncertainties and keeping the solutions that fit within 1σ.

5. Effect of Temperature

Our model of core composition is based on an isentropic (or adiabatic) temperature gradient across the outer core. We fixed the temperature at the ICB of 6300 K, corresponding to the melting point of iron at 330 GPa (14, 15), and extrapolated the temperature at the CMB along the calculated isentrope, to find a CMB temperature of 4300 K.

In order to test the robustness of our prediction, we evaluated the sensitivity of the model temperature. We ran our calculations for a large range of temperatures at the CMB (T_{CMB}), spanning 900 K and bracketing the selected value of 4300 K: from 3800 K (which is a reasonable lower bound) to 4700 K (which is an upper bound). For each T_{CMB}, we calculate a corresponding T_{ICB} following the isentrope, and then again find the compositional solutions that fit the seismological data. As temperature increases, we find that the total amount of light elements diminishes, and more specifically the maximum amount of oxygen and sulfur drops, whereas that of Si and C increases. However, the overall conclusions are unchanged, and the solution we propose for core composition is relatively insensitive to core temperature. The solution from any O-S-Si-C combination that provides the best fit to PREM, is always an O- and Si-bearing core regardless of the core temperature; this is reported in table S2 as a function of temperature.

T_{CMB} (K)	O (wt%)	Si (wt%)	S (wt%)	C (wt%)
3800	4.7	1.7	0	0
4000	4.3	1.8	0	0
4300	3.7	1.9	0	0
4500	3.3	2.1	0	0
4700	3.0	2.2	0	0

Table S2: The best numerical solution (i.e. the one that fits the closest to PREM) for different temperatures at the CMB (main text: T_{CMB}=4300 K, highlighted in yellow). ICB temperatures are calculated on the isentrope for each CMB temperatures. The Fe/Ni ratio is fixed at 16.

We find no quantitative changes: no solutions in the Si-S-C systems, *i.e.* no solutions without oxygen; our central conclusion about the necessity of oxygen in the outer core is preserved over ~1000 K variation in CMB temperature. The best numerical fit is still S- and C-free, and contains between 3.0–4.7 wt% oxygen and 1.7–2.2% silicon (see table S2),. This corroborates the remarkable robustness of our conclusion with respect to uncertainty in CMB temperature. In figure S2, we plotted core compositions (propagating all uncertainties) in the Fe-O-Si, Fe-O-S, and Fe-O-C ternaries; with T_{CMB} ranging from 3800 K to 4700 K, bracketing our standard T_{CMB} of 4300 K.

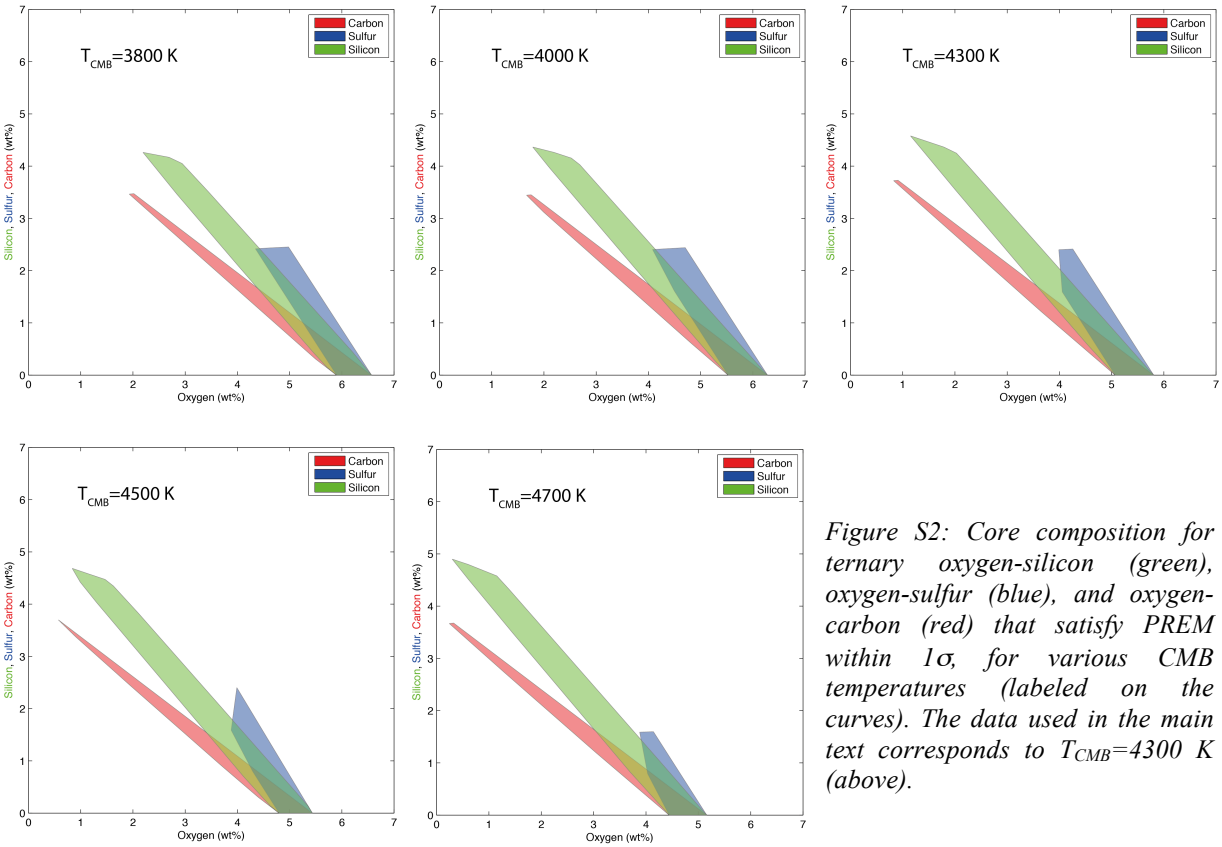

Figure S2: Core composition for ternary oxygen-silicon (green), oxygen-sulfur (blue), and oxygen-carbon (red) that satisfy PREM within 1σ, for various CMB temperatures (labeled on the curves). The data used in the main text corresponds to T_{CMB}=4300 K (above).

6. Effect of Geotherms: adiabatic vs. sub-adiabatic

In our model, we always assumed that the temperature gradient across the outer core was isentropic, and fell on the isentrope of pure iron, as calculated (see section 2 above) self-consistently by our first principles molecular dynamics. This assumes two things: (1) we consider that the outer core is actually adiabatic, and (2) we assume that the adiabat does not change with light elements. Both of these assumptions need to be tested in order to prove the robustness of our compositional model, and both of them result is a sub-adiabatic (less steep) thermal gradient. Firstly, adding light elements should lower the melting temperature with respect to that of pure iron, and therefore that at the ICB resulting in a sub-adiabatic gradient when compared with pure iron. Secondly, the convective outer core could be sub-adiabatic because of solutal convection, and this once again results in a lower temperature at the ICB. So we decided to quantify the effect of 3 different geotherms across the outer core on our composition: pure Fe adiabat, a 300 K sub-adiabatic profile, and a 600 K sub-adiabatic profile.

We kept the temperature at the CMB constant at 4300 K, and used three ICB temperatures of 6300 K (pure Fe adiabat), 6000 K, and 5700 K. The resulting core compositions are in figure S3. Once again, we not small quantitative changes, but qualitatively, as with the change in core temperature, the slope of the core's geotherm makes for minor changes, and our conclusions are unaffected.

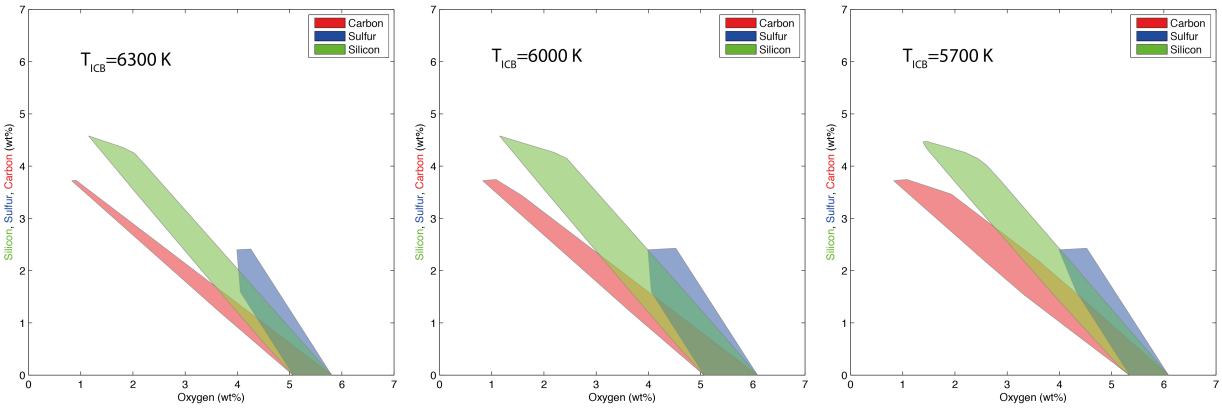

Figure S3: Core composition in ternary oxygen-silicon (green curves), oxygen-sulfur (blue curves), and oxygen-carbon (red curves) that satisfy PREM within 1-σ error, for various geotherms. The temperature at the CMB is fixed (T_{CMB}=4300 K) and we have chosen 3 plausible temperatures at the ICB: T_{ICB}=6300 K (pure Fe adiabat), as well as T_{ICB}=6000 K and T_{ICB}=5700 K corresponding to 300 and 600 K depressions of the adiabat due to light element content and/or solutal convection.

7. References

1. Allègre CJ, Poirier JP, Humler E, & Hofmann AW (1995) The Chemical Composition of the Earth. *Earth and Planetary Science Letters* 134(3-4):515-526.
2. Takafuji N, Hirose K, Mitome M, & Bando Y (2005) Solubilities of O and Si in liquid iron in equilibrium with (Mg,Fe)SiO3 perovskite and the light elements in the core. *Geophysical Research Letters* 32(6).
3. Sakai T*, et al.* (2006) Interaction between iron and post-perovskite at core-mantle boundary and core signature in plume source region. *Geophysical Research Letters* 33(15).
4. Badro J*, et al.* (2007) Effect of light elements on the sound velocities in solid iron: Implications for the composition of Earth's core. *Earth And Planetary Science Letters* 254(1-2):233-238.
5. Huang HJ*, et al.* (2011) Evidence for an oxygen-depleted liquid outer core of the Earth. *Nature* 479(7374):513-U236.
6. Alfe D, Gillan MJ, & Price GD (2002) Composition and temperature of the Earth's core constrained by combining ab initio calculations and seismic data. *Earth and Planetary Science Letters* 195(1-2):91-98.
7. Corgne A, Siebert J, & Badro J (2009) Oxygen as a light element: A solution to single-stage core formation. *Earth And Planetary Science Letters* 288(1-2):108-114.
8. Siebert J, Badro J, Antonangeli D, & Ryerson FJ (2013) Terrestrial Accretion Under Oxidizing Conditions. *Science*.
9. Kresse G & Furthmuller J (1996) Efficient iterative schemes for ab initio total-energy calculations using a plane-wave basis set. *Physical Review B* 54(16):11169-11186.
10. Blöchl PE (1994) Projector Augmented-Wave Method. *Physical Review B* 50(24):17953-17979.
11. Flyvbjerg H (1998) Error estimates on averages of correlated data. *Advances in Computer Simulation,* Lecture Notes in Physics, ed Kertesz JKI), Vol 501, pp 88-103.
12. Cote AS, Vocadlo L, Dobson DP, Alfe D, & Brodholt JP (2010) Ab initio lattice dynamics calculations on the combined effect of temperature and silicon on the stability of different iron phases in the Earth's inner core. *Physics Of The Earth And Planetary Interiors* 178(1-2):2-7.
13. Brown JM & McQueen RG (1986) Phase transitions, Grüneisen parameters and elasticity for shocked iron between 77 GPa and 400 GPa. *Journal of Geophysical Research* 91:7485.
14. Poirier JP (1994) Light-Elements in the Earths Outer Core - a Critical-Review. *Physics of the Earth and Planetary Interiors* 85(3-4):319-337.
15. Anzellini S, Dewaele A, Mezouar M, Loubeyre P, & Morard G (2013) Melting of Iron at Earth's Inner Core Boundary Based on Fast X-ray Diffraction. *Science* 340(6131):464-466.